

Activated Kupffer cells inhibit insulin sensitivity in obese mice

Michaela Tencerova,^{*,1,2} Myriam Aouadi,^{*,2,3,4} Pranitha Vangala,^{*} Sarah M. Nicoloso,^{*} Joseph C. Yawe,^{*} Jessica L. Cohen,^{*} Yuefei Shen,^{*} Lorena Garcia-Menendez,^{*,5} David J. Pedersen,^{*} Karen Gallagher-Dorval,[†] Richard A. Perugini,[†] Olga T. Gupta,^{‡,6} and Michael P. Czech^{*,4}

^{*}Program in Molecular Medicine, [†]Department of Surgery, and [‡]Department of Pediatrics, University of Massachusetts Medical School, Worcester, Massachusetts, USA

ABSTRACT Obesity promotes insulin resistance associated with liver inflammation, elevated glucose production, and type 2 diabetes. Although insulin resistance is attenuated in genetic mouse models that suppress systemic inflammation, it is not clear whether local resident macrophages in liver, denoted Kupffer cells (KCs), directly contribute to this syndrome. We addressed this question by selectively silencing the expression of the master regulator of inflammation, NF- κ B, in KCs in obese mice. We used glucan-encapsulated small interfering RNA particles (GeRPs) that selectively silence gene expression in macrophages *in vivo*. Following intravenous injections, GeRPs containing siRNA against p65 of the NF- κ B complex caused loss of NF- κ B p65 expression in KCs without disrupting NF- κ B in hepatocytes or macrophages in other tissues. Silencing of NF- κ B expression in KCs in obese mice decreased cytokine secretion and improved insulin sensitivity and glucose tolerance without affecting hepatic lipid accumulation. Importantly, GeRPs had no detectable toxic effect. Thus, KCs are key contributors to hepatic insulin resistance in obesity and a potential therapeutic target for metabolic disease.—Tencerova, M., Aouadi, M., Vangala, P., Nicoloso, S. M., Yawe, J. C., Cohen, J. L., Shen, Y., Garcia-Menendez, L., Pedersen, D. J., Gallagher-Dorval, K., Perugini, R. A., Gupta, O. T., Czech, M. P. Activated Kupffer cells inhibit insulin sensitivity in obese mice. *FASEB J.* 29, 000–000 (2015). www.fasebj.org

Key Words: *small interfering RNA · liver macrophages · insulin resistance · hepatic steatosis*

OBESITY IMPAIRS INSULIN RESPONSIVENESS in the liver and is associated with the development of type 2 diabetes with severe comorbid conditions. Although hepatic lipid accumulation (1, 2), endoplasmic reticulum stress (3), and inflammation (4) have all been suggested as potential contributors to obesity-induced insulin resistance, the relative causal roles of these factors are still unclear. For example, nonalcoholic fatty liver disease is a strong known

risk factor for insulin resistance and type 2 diabetes (5), but lipid accumulation in liver can be experimentally dissociated from insulin resistance under certain conditions (6), suggesting that other mechanisms are also involved. Liver macrophages, denoted Kupffer cells (KCs), are thought to be the major source of hepatic inflammation (7); however, their contribution to insulin resistance has not been directly tested because of the lack of technology to manipulate gene expression specifically in KCs. Here we used a new approach to ask whether these immune cells directly contribute to the development of insulin resistance associated with obesity.

To investigate the role of KC activation in obesity-induced insulin resistance, we developed a method to specifically silence gene expression in these hepatic macrophages *in vivo*. This technology is based on small interfering RNA (siRNA) encapsulated within glucan particles derived from baker's yeast, denoted glucan-encapsulated siRNA particles (GeRPs) (8–11). GeRPs loaded with an siRNA against a major regulator of inflammatory cytokine expression, NF- κ B (12, 13), were delivered to KCs of obese mice by intravenous administration. Using this method, we demonstrate that silencing NF- κ B selectively in KCs decreases liver inflammation and improves insulin sensitivity and glucose tolerance in obese mice.

¹ Current affiliation: Molecular Endocrinology & Stem Cell Research Unit, University of Southern Denmark, Odense, Denmark.

² These authors equally contributed to this work.

³ Current affiliation: Integrated Cardio Metabolic Centre, Department of Medicine, Karolinska Institutet, Huddinge, Sweden.

⁴ Correspondence: M.A., Integrated Cardio Metabolic Centre, Department of Medicine Karolinska Institutet, NOVUM, Blickagången 6, 141 57 Huddinge, Sweden. E-mail: myriam.aouadi@ki.se; or M.P.C., Program in Molecular Medicine, Biotech II, Suite 100, University of Massachusetts Medical School, 373 Plantation St., Worcester, MA 01605. E-mail: michael.czech@umassmed.edu

⁵ Current affiliation: Pfizer, Cambridge, MA, USA.

⁶ Current affiliation: Department of Pediatrics, Division of Pediatric Endocrinology, UT Southwestern Medical Center, Dallas, Texas, USA.

doi: 10.1096/fj.15-270496

This article includes supplemental data. Please visit <http://www.fasebj.org> to obtain this information.

Abbreviations: F.C., fold change; FFA, free fatty acid; GeRPs, glucan-encapsulated small interfering RNA particles; GTT, glucose tolerance test; GS, glucan shell; HFD, high-fat diet; KC, Kupffer cell; PTT, pyruvate tolerance test; SCR, scrambled; TG, triglyceride; WT, wild-type

MATERIAL AND METHODS

Animals and diet

Six-week-old male wild-type C57BL/6J (WT) and 5- and 7- to 8-week-old male B6.V-*Lepob/J* (*ob/ob*) mice were (Jackson Laboratory, Bar Harbor, ME, USA) maintained on a 12-hour light/dark cycle. Animals were given free access to food and water. C57BL/6J WT mice were fed a high-fat diet (HFD; 60% calories from lipids; D12492; Research Diets, New Brunswick, NJ, USA) for 14 or 24 weeks beginning at 6 weeks of age. All other mice were fed normal chow diet. All procedures were performed in accordance with protocols approved by the University of Massachusetts Institutional Animal Care and Use Committee.

Human samples

All protocols were approved by the University of Massachusetts Medical School Institutional Review Board. Blood and liver samples were obtained from patients undergoing laparoscopic Roux-en-Y gastric bypass surgery at University of Massachusetts Memorial Medical Center.

GeRP administration by intravenous injection in vivo

GeRPs were prepared as previously described (11). Seven- or 8-week-old genetically obese *ob/ob* mice were treated with 12.5 mg/kg GeRPs loaded with siRNA (247 µg/kg) and Endoport (2.27 mg/kg). Seven-week-old *ob/ob* mice were used for 15-day treatment. They received 2 or 6 doses of fluorescently labeled GeRPs by intravenous injections over 5 or 15 days, respectively. In a model of diet-induced obesity, 6-week-old C57BL/6J mice were fed an HFD for 14 or 24 weeks. They received 6 doses of fluorescently labeled GeRPs for 15 days by intravenous injections.

Isolation of KCs and hepatocytes

The liver of anesthetized mice was first perfused with calcium-free Hanks balanced salt solution, followed by collagenase digestion. After digestion, the hepatocytes were released by dissociation from the lobes and underwent several steps of filtration with calcium plus Hanks balanced salt solution and centrifugation at 50 g for 3 minutes at room temperature. The supernatant from the first centrifugation of hepatocytes was loaded on a Percoll gradient (25% and 50%) and centrifuged for 30 minutes, at 2300 rpm, at 4°C. The interphase ring with KCs was collected and washed 2 times with PBS. The cells were cultured overnight. The following day, primary cells were used for subsequent analyses.

Transfection of primary cells in vitro

Peritoneal exudate cells, isolated as described in Tesz *et al.* (11), and KCs were transfected with the mix of 120 pM siRNA and 3 nM Endoport, which were incubated together for 15 minutes at room temperature before adding to the cells (see **Table 1** for

TABLE 1. List of siRNA sequences used in the study

siRNA	Sequence 5'→3'
Scrambled (SCR)	CAGUCGCGUUUGCGACUGGUU
NF-κB/RelA (2)	GGAUUGAAGAGAAGCGCAAUU

the sequences of siRNAs used in the study). The media were changed 24 hours after transfection and 48 hours after transfection media, mRNA, and protein samples were harvested for subsequent analyses.

Western blot

Cell lysates were separated on an 8% SDS-PAGE polyacrylamide gel, transferred to a PVDF membrane, and incubated overnight at 4°C with primary antibody against p65 (RelA), pSer473 protein kinase B (PKB/AKT), AKT, or actin as a loading control (Cell Signaling, Danvers, MA, USA). Anti-rabbit or anti-mouse IgG antibody conjugated with horseradish peroxidase was used as a secondary antibody. The levels of particular proteins were determined by chemiluminescence (Pierce, Rockford, IL, USA).

Biochemical analyses of TNFα, IL-1β, free fatty acids, triglycerides, aspartate aminotransferase, and alanine aminotransferase

Mouse TNF-α and IL-1β were measured in serum and conditioned media (after 6-hour stimulation with 1 µg/ml LPS) using commercially available kits following the manufacturer's instructions (Thermo Scientific, Waltham, MA, USA). Serum free fatty acid (FFA) and triglyceride (TG) levels in the liver were measured by a commercially available kit (Cayman Chemical, Ann Arbor, MI, USA, and Sigma-Aldrich, Brooklyn, NY, USA, respectively) according to the manufacturer's instructions. Aspartate aminotransferase and alanine aminotransferase levels in serum were measured using a commercial kit (Fisher Scientific, Waltham, MA, USA).

Isolation of RNA and real-time PCR

RNA isolation was performed according to the Trizol Reagent Protocol (Life Technologies, Grand Island, NY, USA). cDNA was synthesized from 0.5 to 1 µg of total RNA using iScript cDNA Synthesis Kit (Bio-Rad, Hercules, CA, USA) according to the manufacturer's instructions. For real-time PCR, synthesized cDNA forward and reverse primers along with the iQ SYBR Green Supermix were run on the CFX96 Real-time PCR System (Bio-Rad). The ribosomal mRNA, 36B4, was used as an internal loading control (see **Table 2** for primer sequences for analyzed genes).

Immunohistochemistry

Cells and tissues were stained using antibodies against F4/80 (AbD Serotec, Raleigh, NC, USA), glial fibrillary acidic protein (R&D Biosystems, Minneapolis, MN, USA), and albumin (Millipore, Billerica, MA, USA) and were analyzed as previously described (8).

Isolation of CD11b+ cells from adipose tissue, blood, and spleen

Adipose tissue stromal vascular fraction, splenic, and blood cells were prepared as described previously (14). The cells were resuspended in 1 ml selection buffer (PBS, 2 mM/L EDTA, and 0.5% bovine serum albumin), and the CD11b-positive cells were selected using CD11b microbeads (Miltenyi, Bergisch Gladbach, Germany), according to the manufacturer's instructions.

Flow cytometry

Cells prepared from liver and spleen were incubated in mouse Fc Block (clone 2.4G2; eBioscience, San Diego, CA, USA) and then stained with specific fluorophore-conjugated primary antibodies

TABLE 2. List of primer sequences used in the study

Genes	Forward sequence 5'→3'	Reverse sequence 5'→3'
Mouse gene		
<i>36B4</i>	TCCAGGCTTTGGGCATCA	CTTTATCAGCTGCACATCACTCAGA
<i>Clec4f</i>	GAGGCCGAGCTGAACAGAG	TGTGAAGCCACCACAAAAGAG
<i>Albumin</i>	TGCTTTTTCCAGGGTGTGTT	TTACTTCCTGCACTAATTTGGCA
<i>NF-κB/RelA</i>	ACTGCCGGGATGGCTACTAT	TCTGGATTCCGCTGGCTAATGG
<i>TNF-α</i>	CCCTCACACTCAGATCATCTTCT	GCTAGCACGTGGGTACAG
<i>IL-1β</i>	GCAACTGTTCCCTGAACTCAACT	ATCTTTTGGGGTCCGTCAACT
<i>IL-6</i>	TAGTCCTTCTACCCCAATTTCC	TTGGTCCTTAGCCACTCCTTC
<i>Srebp-1c</i>	GGAGCCATGGATTGCACATT	GGCCGGGAAGTCACTGT
<i>Chrebp total</i>	CACTCAGGGAATACAGCCTAC	ATCTTGGTCTTAGGGTCTTCAGG
<i>Chrebp α</i>	CGACACTCACCCACCTCTTC	TTGTTTCAGCCGGATCTTGTCT
<i>Chrebp β</i>	TCGCGAGAGCCGCTGGAG	CTTGTCCCGGCATAGCAAC
<i>Elovl6</i>	TCAGCAAAGCAGCCGAAC	AGCGACCATGTCTTTGTAGGAG
<i>Dgat2</i>	GCGCTACTTCCGAGACTACTT	GGGCCTTATGCCAGGAAACT
<i>ACC</i>	TGTACAAGCAGTGTGGGCTGGCT	CCACATGGCCTGGCTTGGAGGG
<i>Acy</i>	ACCCCTTCACTGGGATCACA	GACAGGGATCAGGATTTCTTGT
<i>PPARα</i>	AGAGCCCCATCTGTCTCTCTC	ACTGGTAGTCTGCAAAACCAAA
<i>PPARγ</i>	GGAAGACCACTCGCATTCTCT	GTAATCAGCAACCATTGGGTCA
<i>Fsp27</i>	ATCAGAACAGCCGCAAGAAGA	CAGCTTGTACAGGTGCAAGG
<i>Cidea</i>	ATCACAACTGGCCTGGTTACG	TACTACCCGGTGTCCATTTCT
<i>Fasn</i>	GGAGGTGGTGATAGCCGGTAT	TGGGTAATCCATAGAGCCAG
<i>Scd1</i>	TTCTTGGGATACACTCTGGTGC	CGGGATTGAATGTTCTTGTCTGT
<i>PEPCK</i>	CTGCATAACGGTCTGGACTTC	CAGCAACTGCCCGTACTCC
<i>G6Pase</i>	GTTGAACCAGTCTCCGACCA	CGACTCGCTATCTCCAAGTGA
Human gene		
<i>RPLP0</i>	CAGATTGGCTACCCAACTGTT	GGGAAGGTGTAATCCGTCTCC
<i>TNF-α</i>	ATGAGCACTGAAAGCATGATCC	GAGGGCTGATTAGAGAGAGGTG
<i>IL-1β</i>	CTCGCCAGTGAATGATGGCT	GTGGGAGATTCTGACTGGAT

or isotype control antibodies [F4/80-APC (clone Cl:A3-1); CD11b-PerCP-Cy5.5 (clone M1/70); Gr-1-APC-Cy7 (clone RB6-8C5); Siglec-f-PE (clone E50-2440); Ly6C-PE-Cy7 (clone AL-21); CD3e PE-Cy7 (clone 145-2c11); B220-APC (clone RA3-6B2); BD Biosciences, San Jose, CA, USA]. After staining, the cells were washed 3 times with FACS buffer (1% bovine serum albumin in PBS), and then samples were measured using BD LSRII (BD Biosciences) and analyzed with FlowJo software (TreeStar, Ashland, OR, USA). The gating scheme was designed as previously described (14).

Preparation of glucan shells

Glucan shells (GSs) were prepared as previously described (8). Briefly, β-1,3-D-glucan particles were prepared by suspending *Saccharomyces cerevisiae* (100 g) in 1 L of 0.5 M NaOH and heating to 80°C for 1 h. The insoluble material containing the yeast cell walls was collected by centrifugation, suspended in 1 L of 0.5 M NaOH, and incubated at 80°C for 1 hour. The insoluble residue was again collected by centrifugation and washed 3 times with 1 L of water, 3 times with 200 ml of isopropanol, and 3 times with 200 ml of acetone. The resulting slurry was placed in a glass tray and dried at room temperature to produce 16.2 g of a fine, slightly off-white powder.

Preparation of [¹²⁵I]-GS

Synthesis of tyramine-modified GS—Tyramine residues were conjugated to the GSs using reductive amination chemistry. Briefly, GSs (100 mg) were resuspended in water (7 ml) by sonication. Sodium periodate (22 mg dissolved in 3 ml of water) was added, and the mixture was stirred at 37°C for 24 hours. Oxidized GSs were washed 3 times with water and used immediately for

reductive amination synthesis. Tyramine (135 mg), water (8 ml), and borate buffer (2 ml, 0.1 M, pH 9.5) were added to the oxidized GS samples, and the particles were resuspended and mixed at 37°C overnight. The aminated samples were reduced with sodium borohydride (47 mg) and incubated at room temperature for 48 hours. The reduced samples were washed with water, resuspended in 70% ethanol, and stored overnight at -20°C for sterilization. The particles were isolated by centrifugation, and the particles were resuspended in dd-H₂O. Residual water was removed by lyophilization.

Particle Radiolabeling—For biodistribution and imaging studies, particles were labeled with [¹²⁵I]. All particles were labeled targeting the tyramine residues attached to the GSs. [¹²⁵I] Radionuclide 10⁻⁵ M NaOH (pH 8–11, reductant free; Perkin Elmer, Waltham, MA, USA) was incorporated onto the particles using precoated iodination tubes (Pierce, Rockford, IL, USA) and by following the manufacturer's instructions for the 2-step Chizzone indirect method of labeling. Once iodination was complete, the [¹²⁵I]-GSs were isolated by centrifugation and washed with PBS (9 times) to remove free radionuclide. The specific activity of the final reaction mixture was ~07 μCi/1 mg particles.

[¹²⁵I]-GS biodistribution in vivo

Five-week-old male *ob/ob* mice were intravenously injected with [¹²⁵I]-GS at 407 μCi/1 mg in a volume of 200 μl. A small animal multiple pinhole single-photon emission computed tomography (SPECT/CT) camera (Bioscan, Washington, DC, USA) was used to perform the mouse imaging under isoflurane. The CT and SPECT acquisitions were reconstructed using InVivoScope software. The mice were killed 7 days after injection, and sample tissues were weighed and counted in a NaI(Tl) well counter (Cobra II automatic γ

counter; Packard Instrument Company) along with a standard of the injected material.

Fluorescein labeling of GSs

GSs (1 g) were washed with sodium carbonate buffer (0.1 M, pH 9.2) and resuspended in 0.1 L carbonate buffer. 5-(4,6-Dichlorotriazinyl) aminofluorescein (1 mg/ml in ethanol) was added to the buffered GS suspension [10% (v/v)] and mixed at room temperature in the dark overnight. Tris buffer (2 mM) was added and incubated for 15 minutes, and GSs were washed with sterile pyrogen-free water until the supernatant was clear. The GSs were then flash-frozen and lyophilized in the dark.

Histologic analyses

The paraffin-embedded liver sections were used for hematoxylin-eosin staining and frozen sections of the liver for Oil Red O staining. The pictures were taken by an Axiovert 200 inverted microscope equipped with an AxioCam HR CCD camera (Zeiss, Thornwood, NY, USA).

Metabolic analyses

Glucose and pyruvate tolerance tests (GTTs and PTTs) were performed after GeRP treatment (24 hours after last injection) and 6-hour food withdrawal. A dose of 1 g/kg glucose or pyruvate was intraperitoneally injected, and blood glucose levels were measured by glucometer at defined time points from the tail vein. The following day, the mice were killed to harvest tissues for subsequent analyses.

Insulin-stimulated phosphorylation of AKT *in vivo*

Insulin stimulated phosphorylation of AKT was performed after GeRP treatment (24 hours after last injection) and 4 hours food withdrawal. A dose of 0.75 U/kg insulin was intraperitoneally injected, and then adipose tissue and liver samples were harvested from GeRP-treated mice for subsequent analyses 15 minutes after injection.

Statistical analyses

The data were analyzed using GraphPad 5a software (GraphPad Software, La Jolla, CA, USA). The statistical significance of differences among groups was analyzed using Student *t* test or ANOVA as appropriate. Data were presented as means \pm SEM. $P < 0.05$ was considered statistically significant.

RESULTS

GSs administered by intravenous injection are specifically delivered to KCs *in vivo*

To study GS biodistribution *in vivo*, genetically obese, 5-week-old *ob/ob* mice were intravenously injected with GS radiolabeled with a [¹²⁵I] probe and imaged at different time points using SPECT/CT (see protocol scheme in Fig. 1A). [¹²⁵I]-GSs were mostly found in the liver 24 hours and maintained until at least 7 days after delivery (Fig. 1B). These results were confirmed by flow cytometry analysis

showing high FITC signal in monocytes/macrophages recovered from the liver compared with blood and spleens of *ob/ob* mice 24 hours after intravenous injection (Fig. 1C–E; Supplemental Fig. S1A, B).

Using a protocol developed by our laboratory, we next isolated both hepatocyte and KC fractions from liver 24 hours after FITC-GS intravenous injection (see protocol scheme in Fig. 1F). The purity of both fractions was analyzed by measuring the expression of KC and hepatocyte markers (Fig. 1G). C-type lectin domain family 4, member F (*Clec4f*), was used as a KC marker (15), because it was highly expressed in KCs, whereas it was barely detectable in macrophages isolated from other tissues (Supplemental Fig. S1C). *Alb* was used as a marker for hepatocytes as previously described (16). Fluorescent microscopy showed FITC-GS in KCs but not in hepatocytes or in hepatic stellate cells (stained with an antibody against glial fibrillary acidic protein) in mice intravenously injected with FITC-GS (Fig. 1H; Supplemental Fig. S1D).

Importantly, GeRPs loaded with scrambled (SCR) siRNA had no detectable toxic effect *in vivo*, as serum levels of markers for liver damage, aspartate aminotransferase/alanine aminotransferase, and IL-1 β remained unchanged in mice treated with PBS or SCR-GeRPs (Supplemental Fig. S1E–G). Serum levels of TNF- α were undetectable, and the composition of immune cells in liver was similar with both treatments, as well as mRNA levels of KC marker *Clec4f* (Supplemental Fig. S1H–J). The expression of *Nfkb*, *Il-1 β* , *Tnf α* , and *Il-6* was unchanged in KCs after intravenous delivery of SCR-GeRPs in obese mice (Supplemental Fig. S1K). Taken together, these results show that GeRPs delivered intravenously are mostly found in KCs and do not induce any detectable toxic effect.

Gene silencing in KCs *in vitro*

Consistent with studies showing a correlation between hepatic inflammation and insulin resistance in humans (17), the expression of TNF- α and IL-1 β was increased with insulin resistance in obese patients matched for body mass index (Fig. 2A; Supplemental Fig. S2A for metabolic parameters). TNF- α and IL-1 β expression in the liver was also increased with insulin resistance in *ob/ob* mice (Fig. 2B; see Supplemental Fig. S2B, C for metabolic parameters). In addition, the expression of IL-1 β was 9 times higher in KCs compared with hepatocytes, suggesting KCs as a main source of cytokines (Supplemental Fig. S2D). These results validated *ob/ob* mice as a model to study a causal relationship between inflammation and insulin resistance.

NF- κ B was selected as a target because it had been shown to control the expression of multiple inflammatory cytokines (18), including TNF- α and IL-1 β . First, primary peritoneal macrophages were used to screen for potent siRNAs against the transcriptionally active subunit of NF- κ B, *p65* (Fig. 2C). The most potent siRNA, NF- κ B2, significantly decreased NF- κ B expression at mRNA and protein levels (Fig. 2C). Therefore, this siRNA sequence was selected for subsequent analyses. Similar results were found after transfection of KCs with NF- κ B2 siRNA *in vitro* (Fig. 2D, E). To test the specificity of the siRNA, the protein levels of the ubiquitously and highly expressed ERK1/2

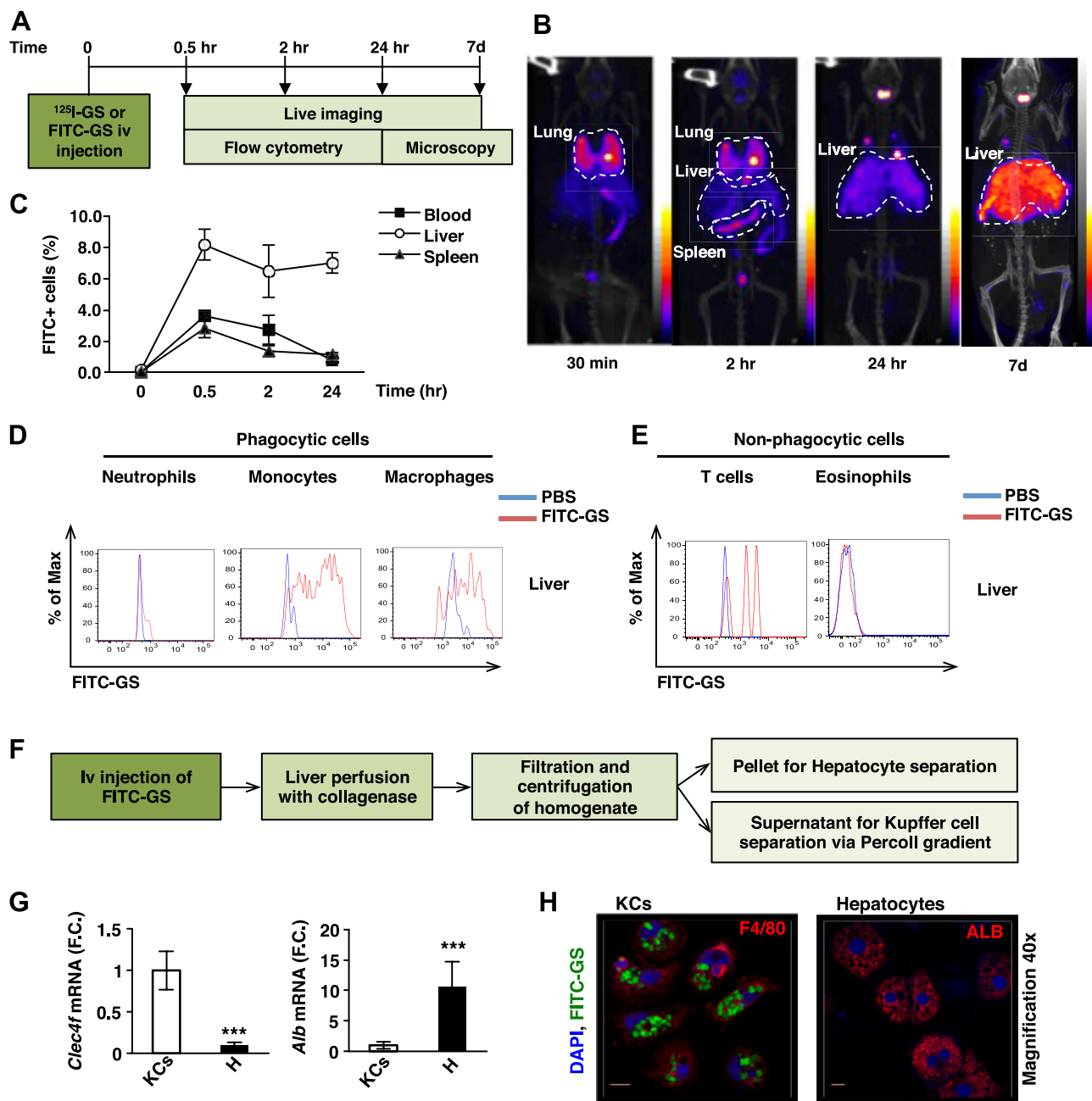


Figure 1. GSs injected intravenously in *ob/ob* mice are mostly localized in liver. **A)** Scheme of protocol design for biodistribution experiment. **B)** Live imaging of 5-week-old *ob/ob* mice intravenously injected with [^{125}I]-GS 30 minutes, 2 hours, 24 hours, and 7 days after injection ($n = 2$). **C)** Flow cytometry analysis of blood, liver, and spleen of *ob/ob* mice intravenously injected with PBS or FITC-GS and harvested at 30 minutes, 2 hours, and 24 hours after injection ($n = 3$ per time point). The data are expressed as the percentage of maximal mean fluorescent intensity. **D)** Profiling of FITC+ signal in phagocytic cells in liver: neutrophils (Gr-1+), monocytes (Ly6-C+), macrophages (F4/80/CD11b+), and **(E)** nonphagocytic cells: T lymphocytes (CD3+) and eosinophils (Siglec-f+) ($n = 3$ per time point). **F)** Scheme of protocol design for KC and hepatocyte isolation. **G)** Expression of *Clec4f* and *Alb* in KC and hepatocyte (H) fractions of 5-week-old *ob/ob* mice ($n = 3-6$). **H)** Confocal microscopy of isolated KCs and hepatocytes ($\times 100$ and $\times 40$ magnification, respectively) from liver of *ob/ob* mice 24 hours after intravenous injection with FITC-labeled GSs. KCs were stained with an antibody against F4/80 (red, left) and hepatocytes with an antibody against albumin (ALB; red, right). Nuclei are stained with DAPI (blue). Scale bar, 10 μm . *** $P < 0.001$. Results are expressed as mean of fold change (F.C.) normalized to KCs expression \pm SEM. Statistical significance was analyzed by Student's *t* test.

were measured in cells treated with SCR or NF- κ B siRNA (Fig. 2E). No change in ERK1/2 protein levels following treatment with NF- κ B compared with SCR was detected, confirming the specificity of the siRNA. Furthermore, the NF- κ B silencing led to significant diminution of expression

of its downstream gene targets (*Il-1 β* , *Tnf α* , and *Il-6*) at both the mRNA and protein levels in peritoneal macrophages and KCs (Fig. 2F-I). These data reveal that NF- κ B can be silenced in peritoneal macrophages and KCs *in vitro* both at the mRNA or protein levels.

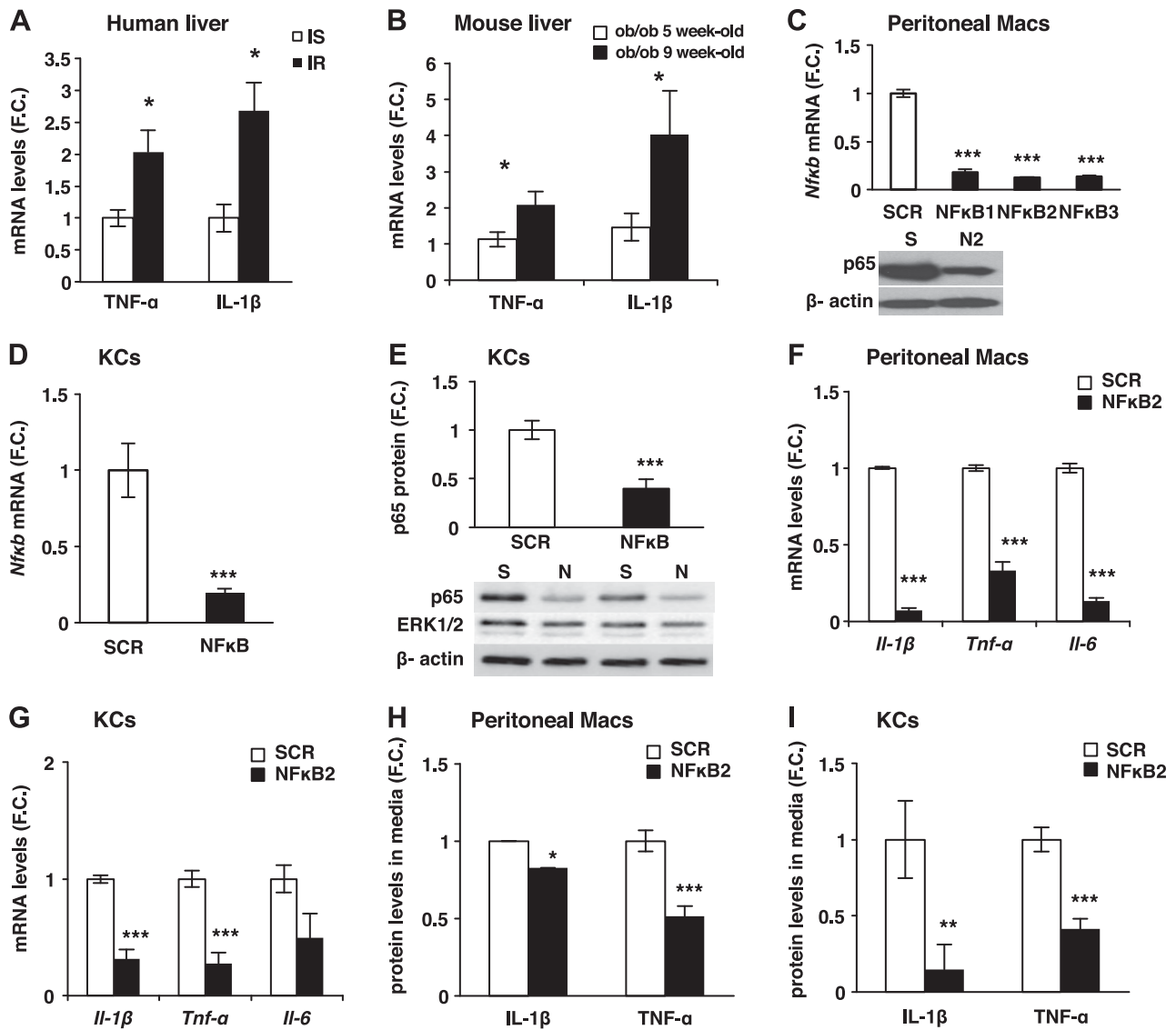


Figure 2. Silencing of *Nfkb* in primary macrophages *in vitro*. A) mRNA levels of inflammatory genes in liver of obese insulin sensitive (IS) or resistant (IR) individuals matched for body mass index ($n = 7$) and (B) 5- or 9-week-old *ob/ob* mice ($n = 5$). C) Peritoneal macrophages isolated from WT mice were treated with 120 pM siRNA (SCR or 3 different sequences of *Nfkb* siRNA) and 3 nM EP for 48 hours. mRNA of *Nfkb* measured by RT-PCR ($n = 4-6$) and representative Western blot of peritoneal macrophages treated with SCR (S) or NF- κ B2 (N2). D) mRNA and (E) protein levels of NF- κ B normalized to β -actin levels and representative Western blot in KCs isolated from WT mice following treatment with siRNA *in vitro*. ERK1/2 was used as a negative control (S, SCR; N, NF- κ B; $n = 7$). F) mRNA expression of *Il-1 β* , *Tnf α* , and *Il-6* measured by RT-PCR in peritoneal macrophages ($n = 4-6$). G) mRNA levels of *Il-1 β* , *Tnf α* , and *Il-6* in KCs following treatment with siRNA *in vitro* ($n = 4-6$). TNF- α and IL-1 β protein levels measured by ELISA in media of (H) peritoneal macrophages and (I) KCs treated with LPS (1 μ g/ml) normalized to RNA concentration ($n = 7-8$). Results are presented as mean of fold change (F.C.) normalized to SCR \pm SEM. * $P < 0.05$, ** $P < 0.01$, *** $P < 0.001$. Statistical significance was analyzed by Student's *t* test.

Specific silencing of *Nfkb* in KCs in obese mice

To test the ability of GeRPs to deliver functional siRNA and silence these genes *in vivo*, 8-week-old *ob/ob* mice were intravenously injected with GeRPs loaded with either SCR or NF- κ B2 siRNA (see protocol scheme in Fig. 3A). After 5 days of GeRP treatment, a significant knockdown of *Nfkb* in KCs was found at both the mRNA and protein levels (Fig. 3B, C). Moreover, GeRP-mediated silencing of *Nfkb* in KCs significantly decreased gene expression of inflammatory cytokines, (*i.e.*, *Il-1 β* and *Tnf α*) (Fig. 3D). Interestingly, there was a significant decrease of IL-1 β secretion induced

by LPS in media of KCs isolated from mice treated with NF- κ B-GeRPs compared with SCR-GeRPs (Fig. 3E). These changes occurred without an effect on the composition of immune cells or the expression of *Clec4f* in the liver of treated mice (Supplemental Fig. S3A–C). As expected, no knockdown of *Nfkb* expression was observed in hepatocytes, which do not contain GeRPs (Fig. 3F).

Because of the important role of adipose tissue inflammation in the regulation of metabolism, we analyzed the GeRP distribution and knockdown in the epididymal adipose tissue. No GeRPs were found in any immune cells isolated from epididymal adipose tissue of mice treated

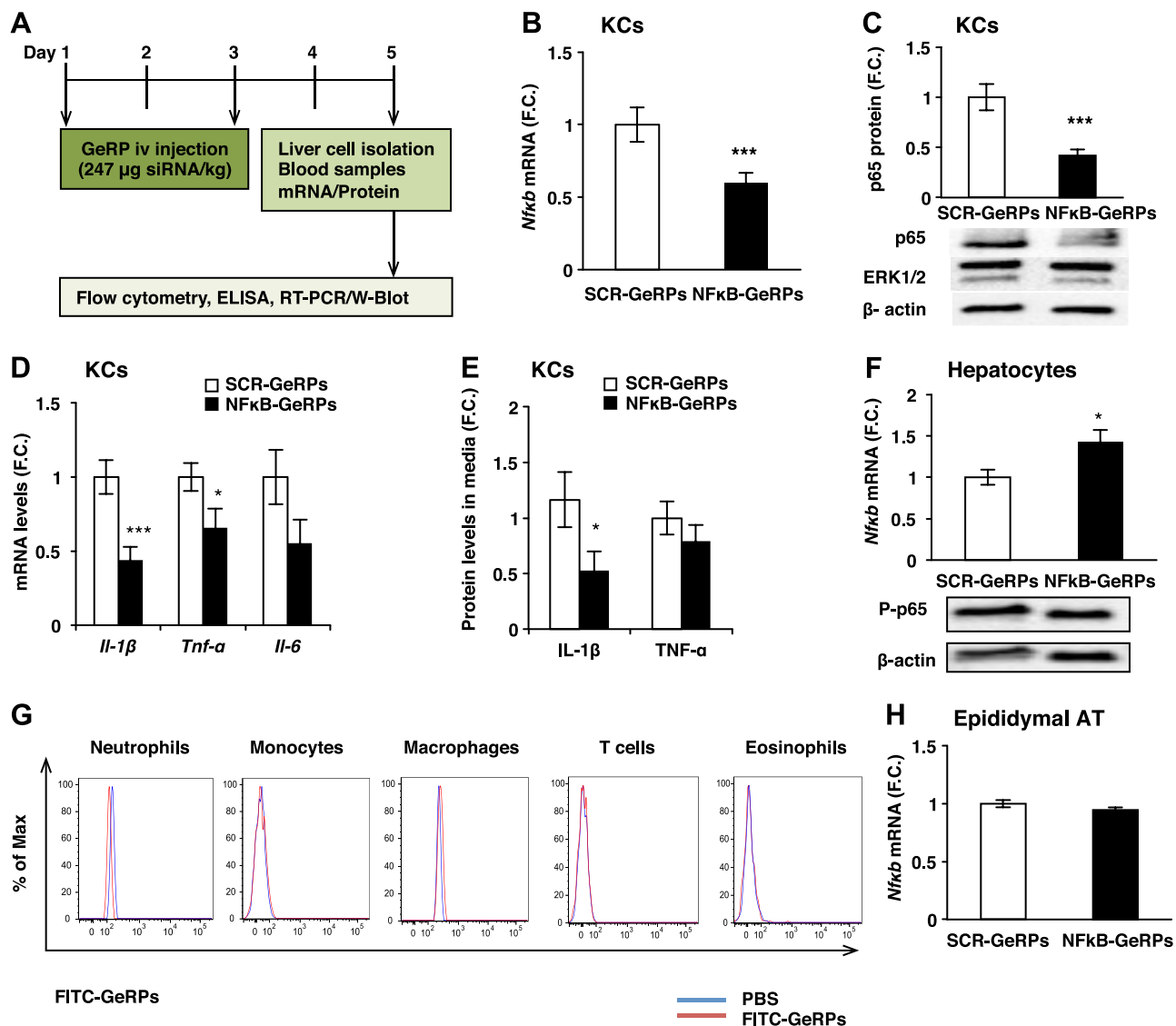


Figure 3. GeRP-mediated silencing of *NfκB* in KCs in *ob/ob* mice. **A**) Protocol of 5-day GeRP treatment in 8-week-old *ob/ob* mice. **B**) mRNA and **(C)** protein levels of NF-κB in KCs isolated from mice treated with either SCR-GeRPs or NF-κB-GeRPs ($n = 11-13$). **D**) mRNA and **(E)** protein levels of *Il-1β*, *Tnfα*, and *Il-6* in KCs of treated mice after LPS stimulation (1 μg/ml). **F**) mRNA and protein levels of NF-κB in hepatocytes ($n = 11-13$). **G**) Flow cytometry analysis on immune cells isolated from epididymal adipose tissue of *ob/ob* mice treated with FITC-GeRPs ($n = 5$). **H**) mRNA levels of *NfκB* in epididymal adipose tissue ($n = 5$). Results are presented as mean of fold change (F.C.) normalized to SCR-GeRPs treated mice \pm SEM. * $P < 0.05$, *** $P < 0.001$. Statistical significance was analyzed by Student's *t* test.

with FITC-GeRPs (Fig. 3G). Consistently, NF-κB-GeRPs administered intravenously did not affect the expression of *NfκB* in epididymal adipose tissue (Fig. 3H). These findings demonstrate that significant gene silencing specifically in KCs can be achieved following GeRP intravenous injection *in vivo* without affecting macrophages in adipose tissue.

Specific silencing of *NfκB* expression in KCs improves insulin sensitivity but has no effect on hepatic steatosis in obese mice

Based on the ability of the intravenously delivered GeRPs to specifically silence genes in KCs but not in other cells or other organs, we assessed the effect of attenuating inflammation in KCs on hepatic lipid accumulation and

insulin resistance in obese mice. Seven-week-old *ob/ob* mice were treated with SCR- or NF-κB-GeRPs for 15 days, and lipid accumulation was assessed at days 5 and 16 (see protocol scheme in Fig. 4A). At both time points, *NfκB* silencing had no effect on lipid accumulation as observed by histologic analyses (hematoxylin-eosin and Oil Red O), TG content, and expression of lipogenic genes (Fig. 4B; Supplemental Fig. S4A–D). In addition, silencing of *NfκB* had no effect on serum FFA levels and total body weight (Supplemental Fig. S4E; data not shown). Taken together, these results show that specific knockdown of *NfκB* in KCs over a 15-day period does not affect hepatic steatosis under our experimental conditions.

To test whether KC activation can affect glucose tolerance, *ob/ob* mice were treated with SCR- or NF-κB-GeRPs for 5 or 15 days, and GTTs were performed at the end of

the treatment (see protocol scheme in Fig. 4A). Although *Nfκb* silencing in KCs showed no effect on glucose tolerance at day 5, we observed a significant improvement at day 16 (Fig. 4C). Consistently, biochemical studies showed an increased insulin-stimulated Akt phosphorylation in liver of mice treated with NF-κB-GeRPs at day 16 (Fig. 4D; Supplemental Fig. S4F), which was accompanied by a decrease in inflammatory gene expression (Supplemental Fig. S4G). We also observed a decrease in basal fasting glycemia in mice after the 15-day treatment compared with 5-day treatment. Although this could be caused by the length of the treatment itself, it could also be explained by the variability in basal glycemia often observed following a short 6-hour fast. Importantly, silencing *Nfκb* specifically in KCs had no effect on insulin-stimulated Akt activation in adipose tissue (Supplemental Fig. S4H). Consistent with the hypothesis that silencing *Nfκb* in KCs improves insulin sensitivity, we observed a significant decrease in the expression of enzymes involved in hepatic glucose production, including phosphoenolpyruvate carboxykinase and glucose 6-phosphatase expression in mice treated with NF-κB-GeRPs compared with SCR-GeRPs (Fig. 4E), which was not observed after 5 day treatment (Supplemental Fig. S4I). The effect of *Nfκb* silencing on insulin sensitivity was independent of an effect on circulating insulin or pancreatic islet mass (Supplemental Fig. S4J, data not shown).

We next studied the effect of NF-κB-GeRPs in a model of diet-induced obesity, which also shows increased liver inflammation (Supplemental Fig. S4K). Six-week-old male C57Bl/6J mice were fed an HFD for 14 or 24 weeks and

treated with SCR- or NF-κB-GeRPs for 15 days (see protocol scheme in Fig. 5A) to study the effect of NF-κB silencing on liver metabolism at different stages of lipid accumulation in the liver. In the 24-week HFD-fed mouse model, GeRP treatment also mediated a significant silencing of *Nfκb* in KCs (Fig. 5B). Furthermore, silencing of *Nfκb* in KCs improved fasting hyperglycemia, glucose tolerance, and lowered hepatic glucose production from pyruvate as measured by PTT (Fig. 5C, D). Importantly, *Nfκb* silencing did not affect body weight or hepatic steatosis (Supplemental Fig. S4L, M). Consistent with this concept, mice fed an HFD for 14 weeks with NF-κB-depleted KCs also exhibited improved glucose tolerance measured by GTT and enhanced insulin-stimulated AKT phosphorylation in the liver independently of TG content (Fig. 5E–H).

DISCUSSION

In the present study, we demonstrated that silencing *Nfκb* specifically in KCs improved insulin sensitivity independent of an effect on total lipid accumulation in diet- or genetically induced obesity. We used the GeRP technology, developed in our laboratory, to deliver siRNA and silence genes specifically in KCs without affecting non-immune cells in the liver and cells in other organs in obese mice. Although various systems have been developed to deliver siRNA to the liver, none of these strategies has demonstrated the ability to specifically target KCs in liver without affecting hepatocytes. Previous studies showing

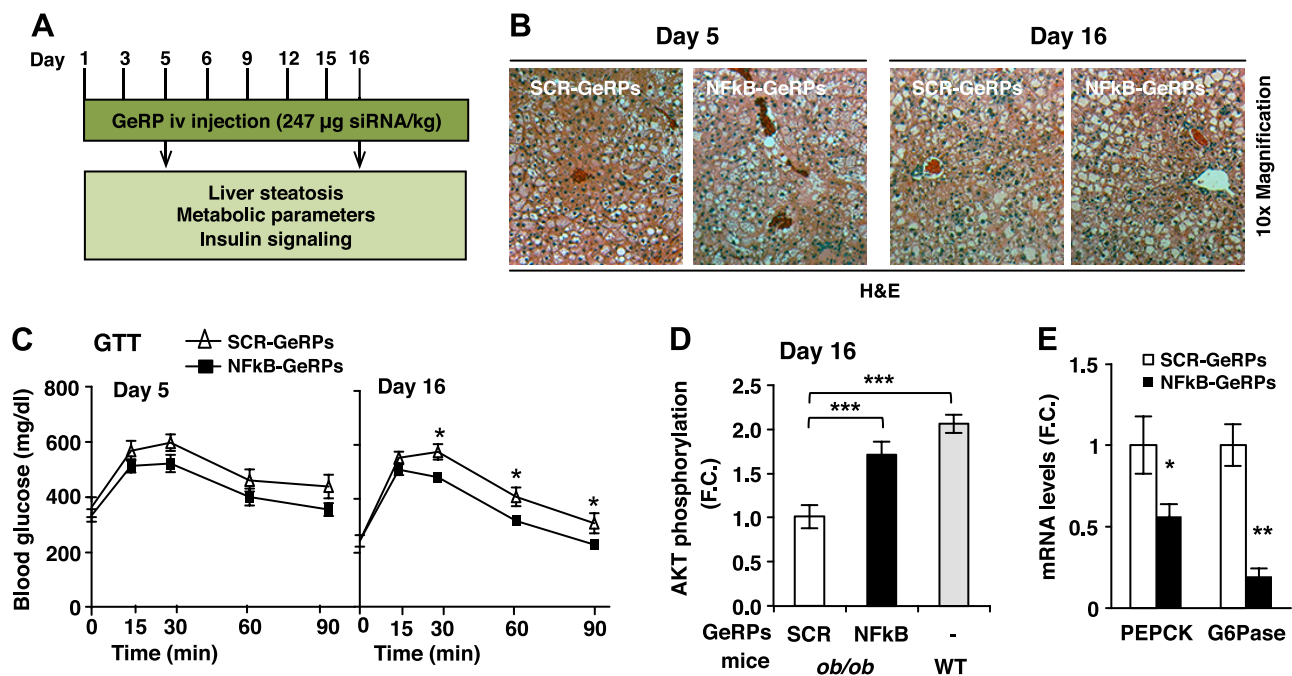


Figure 4. Silencing of *Nfκb* in KCs in *ob/ob* mice improves glucose tolerance without affecting liver steatosis. A) Protocol of 5- and 15-day GeRP treatment. 8-week-old mice were used for the 5-day treatment and 7-week-old mice were used for the 15-day treatment. B) Hematoxylin-eosin liver sections from mice treated with SCR- or NF-κB-GeRPs and (C) GTT (1 g/kg) were performed on mice treated with SCR- or NF-κB-GeRPs after withholding food for 6 hours. D) F.C. of Akt phosphorylation by insulin measured by densitometry of pSer473-Akt normalized to total Akt (*ob/ob*, *n* = 9–10; WT, *n* = 3). E) mRNA levels of gluconeogenic genes in liver from mice treated for 15 days with SCR- or NF-κB-GeRPs (*n* = 5). Results are presented as mean of fold change (F.C.) normalized to SCR-GeRPs-treated mice ± SEM. **P* < 0.05; ***P* < 0.01. The statistical significance was analyzed by *t* test or ANOVA followed by Tukey posttest.

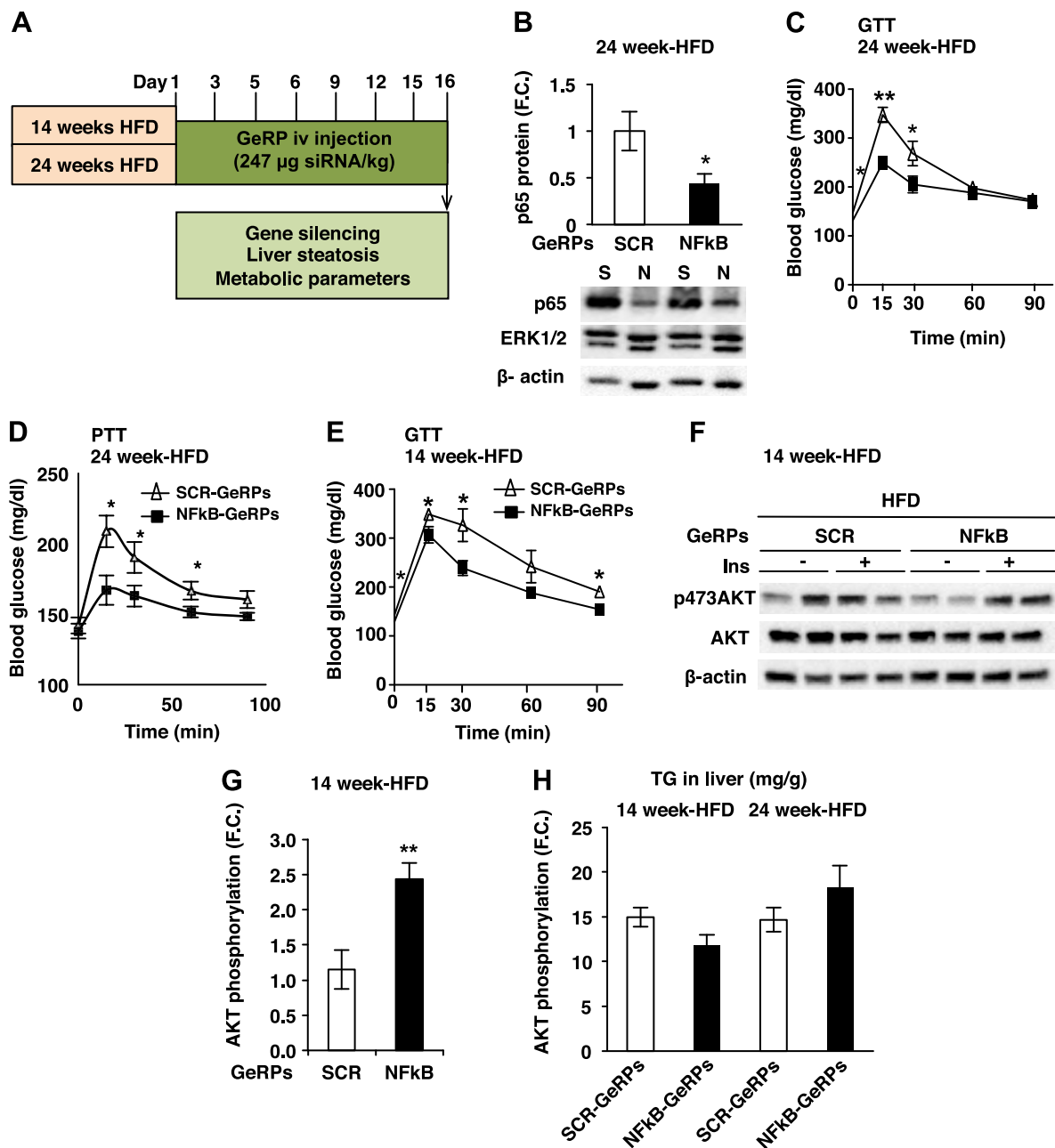


Figure 5. GeRP-mediated silencing of *Nfκb* in KCs in mice fed a HFD improves glucose tolerance. *A*) Protocol of GeRP treatment in mice fed an HFD for 14 or 24 weeks. *B*) Representative Western blot and protein levels of NF-κB normalized to β-actin levels in KCs following a 15-day GeRP treatment in mice fed 24 weeks of an HFD. ERK1/2 was used as a negative control (S, SCR; N, NF-κB; $n = 5$). *C*) GTT (1 g/kg) was performed in mice fed 24 weeks of an HFD and treated with SCR- or NF-κB-GeRPs ($n = 11-14$). *D*) PTT (1 g/kg) was performed in mice fed a 24-week HFD treated with SCR- or NF-κB-GeRPs after withholding food for 6 hours ($n = 5$). *E*) GTT (1 g/kg) was performed in mice fed a 14-week HFD and treated with SCR- or NF-κB-GeRPs ($n = 11-14$). *F*) Representative Western blot of total and activated (pSer473) Akt in the liver of 14-week HFD mice. *G*) F.C. of Akt phosphorylation by insulin measured by densitometry of pSer473-Akt normalized to total Akt ($n = 9-10$). *H*) TG content in the liver ($n = 5$). Results are presented as mean of F.C. normalized to SCR-GeRPs-treated mice \pm SEM. * $P < 0.05$; ** $P < 0.01$; *** $P < 0.001$. The statistical significance was analyzed by *t* test or ANOVA followed by Tukey posttest.

siRNA delivery to KCs *in vivo* used carriers that were also internalized by nonphagocytic cells or phagocytic cells in organs other than liver (19–24). In the present study, we accomplished specific delivery of GSs to KCs in obese mice by taking advantage of the micrometer-size and Dectin 1 receptor-mediated recognition of GS (11). Importantly,

because GeRP treatment did not induce liver toxicity, it represents a major advantage over methods previously used, such as KC depletion (25, 26), to study the role of inflammation genes expressed by KCs in liver diseases.

In our study, we demonstrated that GeRP-mediated silencing of *Nfκb* in KCs decreased the expression of *Nfκb*

and its downstream targets: *Il-1 β* and *Tnf- α* . Interestingly, silencing *Nf- κ b* had no effect on the expression of another inflammatory cytokine, *Il-6*, known to be also regulated by other pathways, such as JNK (27, 28). Consistent with the lack of effect of *Nf- κ b* silencing on *Il-6* expression, JNK protein levels and activation induced by LPS were not affected by *Nf- κ b* silencing in primary macrophages (data not shown).

Several studies have investigated the role of KCs in insulin resistance and hepatic steatosis in obese mice. These studies used systemic delivery of anti-inflammatory drugs, bone marrow transplantation, or transgenic mice deficient in inflammatory genes, which had inhibitory effects on both hepatic steatosis and insulin resistance (12, 26, 27, 29), making it difficult to dissect the specific role of lipid accumulation vs. inflammation in the development of insulin resistance. Based on the finding that *Nf- κ b* silencing in KCs had no effect on total hepatic lipid accumulation in obese mice, we were able to study the direct role of KCs in the development of insulin resistance independently of hepatic steatosis. Our data demonstrate that silencing *Nf- κ b* in KCs improves insulin sensitivity in obese mice.

Multiple studies have reported a beneficial effect of systemic inhibition of NF- κ B on the development of hepatic steatosis (13, 29–31). Similarly, whole body knockout of an upstream activator of NF- κ B, IKK ϵ , reduced liver inflammation and steatosis (30). One possible reason for the lack of effect on hepatic steatosis in our model could be the incomplete depletion of NF- κ B attained under our conditions. However, other points could explain the discrepancy between these studies and our report. First, in our model, *Nf- κ b* is not silenced in cells other than KCs. According to several studies, NF- κ B expressed by hepatocytes plays an important role in hepatic steatosis (13). Second, the observed effects in previous reports may also be the result of inhibiting NF- κ B in tissues other than liver, such as adipose tissue, which indirectly affects hepatic steatosis. Indeed, because hepatic steatosis is in part caused by the inability of adipose tissue to store lipids (5), systemic inhibition of NF- κ B could lower lipid accumulation in liver by decreasing lipolysis and circulating FFAs. In our model, NF- κ B-GeRPs administered intravenously did not affect the levels of serum FFAs or the expression of *Nf- κ b* in adipose tissue. Third, in our model, a sustained inhibition of NF- κ B may be needed to achieve a reduction in liver steatosis. We silenced *Nf- κ b* for 5–15 d, whereas small molecules, including inhibitor of IKK2 and salicylates, were administered for \geq 4 weeks (29, 31, 32). Fourth, in all previous studies, systemic inhibition of NF- κ B is accompanied by weight loss, which has been shown to reduce liver lipid content. However, no effect on body weight was observed in our model following *Nf- κ b* silencing with GeRPs. Finally, we silenced the expression of *Nf- κ b* in mice that were already obese with severe liver damage, whereas the inhibition of NF- κ B in the studies mentioned above was concomitant to the development of obesity and hepatic steatosis.

Importantly, silencing *Nf- κ b* for 15 days resulted in a significant improvement of insulin sensitivity, measured by GTT, and increased AKT phosphorylation in the liver in *ob/ob* and HFD mice. Our findings are consistent with data from the literature showing dissociation of hepatic steatosis from insulin resistance (33, 34). Furthermore, *Nf- κ b* has been shown to be significantly decreased in mice

overexpressing carbohydrate response element binding protein (*ChREBP*) in hepatocytes, which also exhibit an increased hepatic steatosis but improved glucose metabolism in the liver (33). Although additional work would be needed to unravel the cross-talk between KCs and parenchymal cells and its impact on liver diseases, the GeRP technology provides a unique tool for such studies.

Together, these data demonstrate that partial silencing of *Nf- κ b* specifically in KCs improves insulin sensitivity independent of an effect on total lipid accumulation in diet- or genetically induced obesity under our experimental conditions. Thus, KC activation and consequent liver inflammation play causal roles in the development of insulin resistance in mouse models of obesity. **FJ**

The authors thank members of their laboratory group for excellent discussion. The authors appreciate the help of Mary Ruszkowski and Miles Smith at the small animal imaging core, and the staff of the Flow Cytometry Core, the Morphology Core, and Paul Furciniti for the spinning disk confocal microscopy at the University of Massachusetts (UMASS) Medical School. These studies were supported by grants to M.P.C. from the U.S. National Institutes of Health (NIH) National Institute of Diabetes and Digestive and Kidney Diseases (NIDDK; DK085753 and DK030898), NIH National Institute of Allergy and Infectious Diseases (AI046629), and the International Research Alliance of the Novo Nordisk Foundation Center for Metabolic Research. The Morphology Core Facility at the UMASS Medical School Diabetes and Endocrinology Research Center, funded by NIH NIDDK Grant DK325220 is also gratefully acknowledged. J.L.C. is supported by the NIDDK under a Ruth L. Kirschstein National Research Service Award (NRSA) postdoctoral fellowship (F32DK098879). J.C.Y. is supported by a predoctoral NRSA from the NIH NIDDK (DK096948-02). The authors declare no conflicts of interest.

REFERENCES

1. Chavez, J. A., and Summers, S. A. (2012) A ceramide-centric view of insulin resistance. *Cell Metab.* **15**, 585–594
2. Samuel, V. T., and Shulman, G. I. (2012) Mechanisms for insulin resistance: common threads and missing links. *Cell* **148**, 852–871
3. Fu, S., Watkins, S. M., and Hotamisligil, G. S. (2012) The role of endoplasmic reticulum in hepatic lipid homeostasis and stress signaling. *Cell Metab.* **15**, 623–634
4. Glass, C. K., and Olefsky, J. M. (2012) Inflammation and lipid signaling in the etiology of insulin resistance. *Cell Metab.* **15**, 635–645
5. Perry, R. J., Samuel, V. T., Petersen, K. F., and Shulman, G. I. (2014) The role of hepatic lipids in hepatic insulin resistance and type 2 diabetes. *Nature* **510**, 84–91
6. Sun, Z., and Lazar, M. A. (2013) Dissociating fatty liver and diabetes. *Trends Endocrinol. Metab.* **24**, 4–12
7. Ramadori, G., and Armbrust, T. (2001) Cytokines in the liver. *Eur. J. Gastroenterol. Hepatol.* **13**, 777–784
8. Aouadi, M., Tencerova, M., Vangala, P., Yawe, J. C., Nicoloso, S. M., Amano, S. U., Cohen, J. L., and Czech, M. P. (2013) Gene silencing in adipose tissue macrophages regulates whole-body metabolism in obese mice. *Proc. Natl. Acad. Sci. USA* **110**, 8278–8283
9. Aouadi, M., Tesz, G. J., Nicoloso, S. M., Wang, M., Chouinard, M., Soto, E., Ostroff, G. R., and Czech, M. P. (2009) Orally delivered siRNA targeting macrophage Map4k4 suppresses systemic inflammation. *Nature* **458**, 1180–1184
10. Jourdan, T., Godlewski, G., Cinar, R., Bertola, A., Szanda, G., Liu, J., Tam, J., Han, T., Mukhopadhyay, B., Skarulis, M. C., Ju, C., Aouadi, M., Czech, M. P., and Kunos, G. (2013) Activation of the Nlrp3 inflammasome in infiltrating macrophages by endocannabinoids mediates beta cell loss in type 2 diabetes. *Nat. Med.* **19**, 1132–1140

11. Tesz, G. J., Aouadi, M., Prot, M., Nicoloso, S. M., Boutet, E., Amano, S. U., Goller, A., Wang, M., Guo, C. A., Salomon, W. E., Virbasius, J. V., Baum, R. A., O'Connor, M. J., Jr., Soto, E., Ostroff, G. R., and Czech, M. P. (2011) Glucan particles for selective delivery of siRNA to phagocytic cells in mice. *Biochem. J.* **436**, 351–362
12. Arkan, M. C., Hevener, A. L., Greten, F. R., Maeda, S., Li, Z. W., Long, J. M., Wynshaw-Boris, A., Poli, G., Olefsky, J., and Karin, M. (2005) IKK-beta links inflammation to obesity-induced insulin resistance. *Nat. Med.* **11**, 191–198
13. Cai, D., Yuan, M., Frantz, D. F., Melendez, P. A., Hansen, L., Lee, J., and Shoelson, S. E. (2005) Local and systemic insulin resistance resulting from hepatic activation of IKK-beta and NF-kappaB. *Nat. Med.* **11**, 183–190
14. Amano, S. U., Cohen, J. L., Vangala, P., Tencerova, M., Nicoloso, S. M., Yawe, J. C., Shen, Y., Czech, M. P., and Aouadi, M. (2014) Local proliferation of macrophages contributes to obesity-associated adipose tissue inflammation. *Cell Metab.* **19**, 162–171
15. Yang, C. Y., Chen, J. B., Tsai, T. F., Tsai, Y. C., Tsai, C. Y., Liang, P. H., Hsu, T. L., Wu, C. Y., Netea, M. G., Wong, C. H., and Hsieh, S. L. (2013) CLEC4F is an inducible C-type lectin in F4/80-positive cells and is involved in alpha-galactosylceramide presentation in liver. *PLoS ONE* **8**, e65070
16. Lian, G., Wang, C., Teng, C., Zhang, C., Du, L., Zhong, Q., Miao, C., Ding, M., and Deng, H. (2006) Failure of hepatocyte marker-expressing hematopoietic progenitor cells to efficiently convert into hepatocytes in vitro. *Exp. Hematol.* **34**, 348–358
17. Bertola, A., Bonnafous, S., Anty, R., Patouraux, S., Saint-Paul, M. C., Iannelli, A., Gugenheim, J., Barr, J., Mato, J. M., Le Marchand-Brustel, Y., Tran, A., and Gual, P. (2010) Hepatic expression patterns of inflammatory and immune response genes associated with obesity and NASH in morbidly obese patients. *PLoS ONE* **5**, e13577
18. Oeckinghaus, A., Hayden, M. S., and Ghosh, S. (2011) Crosstalk in NF-κB signaling pathways. *Nat. Immunol.* **12**, 695–708
19. Dolina, J. S., Sung, S. S., Novobrantseva, T. I., Nguyen, T. M., and Hahn, Y. S. (2013) Lipidoid Nanoparticles Containing PD-L1 siRNA Delivered In Vivo Enter Kupffer Cells and Enhance NK and CD8(+) T Cell-mediated Hepatic Antiviral Immunity. *Mol Ther Nucleic Acids* **2**, e72
20. Hoffmann, F., Sass, G., Zillies, J., Zahler, S., Tiegs, G., Hartkorn, A., Fuchs, S., Wagner, J., Winter, G., Coester, C., Gerbes, A. L., and Vollmar, A. M. (2009) A novel technique for selective NF-kappaB inhibition in Kupffer cells: contrary effects in fulminant hepatitis and ischaemia-reperfusion. *Gut* **58**, 1670–1678
21. Jing, Y., Shishkov, A., and Ponnappa, B. C. (2008) Inhibition of tumor necrosis factor alpha secretion in rat Kupffer cells by siRNA: in vivo efficacy of siRNA-liposomes. *Biochim. Biophys. Acta* **1780**, 34–40
22. Lee, S., Yang, S. C., Kao, C. Y., Pierce, R. H., and Murthy, N. (2009) Solid polymeric microparticles enhance the delivery of siRNA to macrophages in vivo. *Nucleic Acids Res.* **37**, e145
23. Ogushi, I., Imuro, Y., Seki, E., Son, G., Hirano, T., Hada, T., Tsutsui, H., Nakanishi, K., Morishita, R., Kaneda, Y., and Fujimoto, J. (2003) Nuclear factor kappa B decoy oligodeoxynucleotides prevent endotoxin-induced fatal liver failure in a murine model. *Hepatology* **38**, 335–344
24. Tosello-Tramont, A. C., Landes, S. G., Nguyen, V., Novobrantseva, T. I., and Hahn, Y. S. (2012) Kupffer cells trigger nonalcoholic steatohepatitis development in diet-induced mouse model through tumor necrosis factor-α production. *J. Biol. Chem.* **287**, 40161–40172
25. Clementi, A. H., Gaudy, A. M., van Rooijen, N., Pierce, R. H., and Mooney, R. A. (2009) Loss of Kupffer cells in diet-induced obesity is associated with increased hepatic steatosis, STAT3 signaling, and further decreases in insulin signaling. *Biochim. Biophys. Acta* **1792**, 1062–1072
26. Stienstra, R., Saudale, F., Duval, C., Keshtkar, S., Groener, J. E., van Rooijen, N., Staels, B., Kersten, S., and Müller, M. (2010) Kupffer cells promote hepatic steatosis via interleukin-1beta-dependent suppression of peroxisome proliferator-activated receptor alpha activity. *Hepatology* **51**, 511–522
27. Han, M. S., Jung, D. Y., Morel, C., Lakhani, S. A., Kim, J. K., Flavell, R. A., and Davis, R. J. (2013) JNK expression by macrophages promotes obesity-induced insulin resistance and inflammation. *Science* **339**, 218–222
28. Thobe, B. M., Frink, M., Hildebrand, F., Schwacha, M. G., Hubbard, W. J., Choudhry, M. A., and Chaudry, I. H. (2007) The role of MAPK in Kupffer cell toll-like receptor (TLR) 2-, TLR4-, and TLR9-mediated signaling following trauma-hemorrhage. *J. Cell. Physiol.* **210**, 667–675
29. Beraza, N., Malato, Y., Vander Borgh, S., Liedtke, C., Wasmuth, H. E., Dreano, M., de Vos, R., Roskams, T., and Trautwein, C. (2008) Pharmacological IKK2 inhibition blocks liver steatosis and initiation of non-alcoholic steatohepatitis. *Gut* **57**, 655–663
30. Chiang, S. H., Bazuine, M., Lumeng, C. N., Geletka, L. M., Mowers, J., White, N. M., Ma, J. T., Zhou, J., Qi, N., Westcott, D., Delproposto, J. B., Blackwell, T. S., Yull, F. E., and Saltiel, A. R. (2009) The protein kinase IKKepsilon regulates energy balance in obese mice. *Cell* **138**, 961–975
31. Reilly, S. M., Chiang, S. H., Decker, S. J., Chang, L., Uhm, M., Larsen, M. J., Rubin, J. R., Mowers, J., White, N. M., Hochberg, I., Downes, M., Yu, R. T., Liddle, C., Evans, R. M., Oh, D., Li, P., Olefsky, J. M., and Saltiel, A. R. (2013) An inhibitor of the protein kinases TBK1 and IKKε improves obesity-related metabolic dysfunction in mice. *Nat. Med.* **19**, 313–321
32. Yuan, M., Konstantopoulos, N., Lee, J., Hansen, L., Li, Z. W., Karin, M., and Shoelson, S. E. (2001) Reversal of obesity- and diet-induced insulin resistance with salicylates or targeted disruption of Ikkbeta. *Science* **293**, 1673–1677
33. Benhamed, F., Denechaud, P. D., Lemoine, M., Robichon, C., Moldes, M., Bertrand-Michel, J., Ratziu, V., Serfaty, L., Housset, C., Capeau, J., Girard, J., Guillou, H., and Postic, C. (2012) The lipogenic transcription factor ChREBP dissociates hepatic steatosis from insulin resistance in mice and humans. *J. Clin. Invest.* **122**, 2176–2194
34. Moon, Y. A., Liang, G., Xie, X., Frank-Kamenetsky, M., Fitzgerald, K., Kotliansky, V., Brown, M. S., Goldstein, J. L., and Horton, J. D. (2012) The Scap/SREBP pathway is essential for developing diabetic fatty liver and carbohydrate-induced hypertriglyceridemia in animals. *Cell Metab.* **15**, 240–246

Received for publication January 21, 2015.

Accepted for publication March 5, 2015.